

Figure 1. NMR (^{13}C , 22.63 MHz) C_1 of propyllithium-1- ^{13}C -1- ^6Li , 0.5 M in cyclopentane at several temperatures.

Table I. ^{13}C NMR Data for Intermediates

compd	$\delta(1)^a$	$\delta(2)$	$\delta(3)$	$J(1,2)^b$
1	180.9	27.40	8.7	55.5
2	65.53	25.84	10.14	39.6
3	46.99	26.11	11.65	35.4

^a Parts per million from Me_4Si . ^b Hertz.

intensity at the expense of the others and by 270 K this represents the main species present. Also above 210 K there is line broadening and coalescence indicative of some exchange process involving ^6Li taking place on the NMR time scale.

Comparison of the relative peak areas in the ^{13}C and ^6Li spectra, Figures 2-4, reveals that there is a 1:1 correspondence between the summed areas of peaks C, D, and E in the ^6Li spectra and the total area of C, D, and E in the ^{13}C spectra. Also peaks A and B in the ^6Li spectra correspond to A and B, respectively, in the ^{13}C spectrum. These peaks may be assumed to come from different propyllithium aggregates. Thus, each aggregate gives one ^6Li peak and one for ^{13}C ; see Table II.

Next, let us consider the significance of the splittings due to ^{13}C - ^6Li coupling observed in the ^{13}C NMR spectra. Most *n*-alkyllithiums in hydrocarbon solvents at 270-320 K consist of hexamers² with most likely an octahedral structure.¹² So the upfield resonance, A, for C_1 , which is the predominant one at higher temperatures, probably represents a hexamer. In this structure, each C_1 is symmetrically flanked by three ^6Li 's. Thus, the ^{13}C NMR spectrum for C_1 should consist of a seven-line multiplet with relative intensities 1:3:6:7:6:3:1. But, in fact, one sees 9-11 lines whose intensity ratios are more consistent with a fluxional hexamer wherein each $^{13}\text{C}_1$ is coupled on the average equally to all six lithiums (^6Li). That would give, for C_1 , 13 lines, 1:6:21:50:90:126:140:126:90:50:21:6:1, of which we miss two to four lines due to their predicted weak intensities. If this interpretation is correct, the 3.35-Hz splitting observed for this high-field multiplet represents the average of three nearest-neighbor ^{13}C - ^6Li couplings with three couplings to the more distant lithiums in the back of the octahedron, the dotted triangle in 6. We can assume

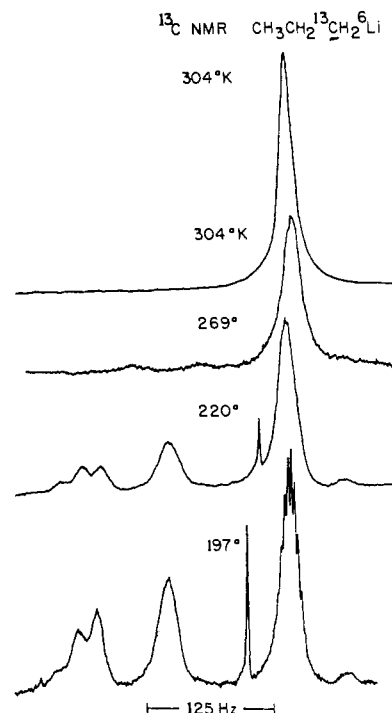
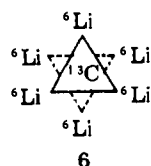


Figure 2. NMR (^{13}C , 67.89 MHz) C_1 of 4, 0.5 M in cyclopentane.

Table II

K	peak		
	E + D + C	B	A
A. Relative Areas of Peaks A-E ^a in ^6Li NMR Spectrum of 4, 0.5 M in Cyclopentane, 39.73 MHz, at Different Temperatures			
181	0.48	0.22	0.30
195	0.37	0.24	0.39
212	0.36		0.64
227	0.22		0.77
246	0.18		0.82
B. Relative Areas of Peaks A-E ^b in ^{13}C NMR Spectrum of 4, 0.5 M in Cyclopentane, 67.89 MHz, at Different Temperatures			
179	0.40	0.30	0.30
197	0.37	0.25	0.38
211	0.30	0.70	
226	0.18	0.82	
239	0.16	0.84	
253	0.13	0.87	

^a See Figure 4. ^b See Figure 3.

the long-range coupling constants to be very small so the directly bonded $J(^{13}\text{C}-^6\text{Li})$ is ca. 6.7 Hz in the hexamer. Translated to $J(^{13}\text{C}-^7\text{Li})$ this would be 17.7 Hz, not much different from the values for methylithium⁷ and butyllithium⁸ in ether of 14.7 and 15 Hz, respectively. These are known to be couplings around a four-center symmetrical C_1 - Li_3 bond in the tetrameric etherates.

By analogy to the hexamer all the aggregates in the system could be fluxional. If the 6.7-Hz nearest-neighbor ^{13}C - ^6Li coupling applies to them also, then the observed splittings result from averaging three couplings of 6.7 Hz over different numbers of lithiums; i.e., the splitting is $3 \times 6.7/n$ where *n* is the association number. The result is that peaks C and D in the ^{13}C NMR spectrum represent nonamers while B applies to an octamer. Peak E, though weak, also shows the nonamer splitting; see Table III.

Aggregation numbers for alkyllithium compounds above six are not well known. However, the conclusions discussed

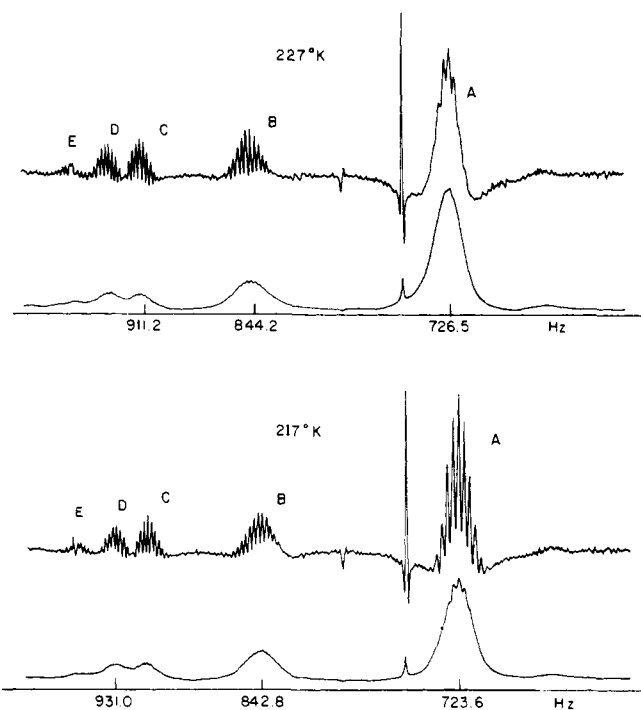


Figure 3. NMR (^{13}C , 67.89 MHz) C_1 of **4**, 0.5 M, cyclopentane, at two temperatures with resolution enhancement.

above are reinforced by the results of ^{13}C T_1 measurements at 192 K using a 0.9 M solution of **4** in cyclopentane. The values of $1/T_1$ for peaks A, B, and C are 2.40 ± 0.03 , 4.10 ± 0.38 , and $3.67 \pm 0.44 \text{ s}^{-1}$ (least-squares fit), respectively. Since $1/T_1$ is proportional to the correlation time for isotropically rotating molecules, the larger $1/T_1$ values correspond to the higher association numbers. These come from the same resonances which prevail at lower temperatures. One of the few studies of alkyllithium association at low temperature using hydrocarbon solvents revealed association numbers exceeding six for 2-methylbutyllithium at 255 K.⁴ The known variation in chemical behavior of alkyllithiums with temperature may also be the result of changes in aggregation.³

Further details about equilibria among aggregates of *n*-propyllithium are revealed by use of ^{13}C peak areas for different concentrations of this reagent at different temperatures, together with the derived association numbers given in Table III. Table IV lists equilibrium constants $K_{x,y}$, defined for the system of equilibria as



where *x,y* are aggregates and *m,n* their respective association numbers. The experimental results are consistent with the system of equilibria, (1), with a least-squares deviation of 10%, which is satisfactory considering the assumptions taken and inherent experimental errors. The temperature dependence of these results gives thermodynamic data in Table V.

The NMR spectra described above also provide information on the dynamic behavior of propyllithium. The narrowing which takes place at the higher temperatures in the ^{13}C NMR of **4** is clearly the result of fast interaggregate carbon–lithium bond exchange. The new resonances which develop downfield of that for the hexamer only become significant below 240 K. By this temperature interaggregate carbon–lithium bond exchange is too slow to change the frequencies of all these resonances. Exchange affects only the line shapes. The onset of splitting in peaks A–E takes place at quite different temperatures, and each peak broadens out again at a lower set of temperatures, all different. This behavior implies that the in-

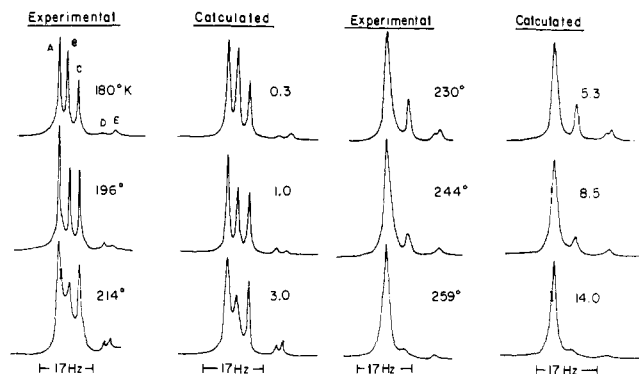


Figure 4. NMR (^6Li , 39.73 MHz) *n*-propyllithium- ^6Li , 0.6 M in cyclopentane, at different temperatures with calculated line shapes and rate constants.

Table III. Association Numbers,^a *n*, of Propyllithium in Cyclopentane from ^{13}C NMR

peak no.	E	D	C	B	A
exptl splitting $\pm 0.07 \text{ Hz}$	2.22	2.22	2.22	2.48	3.35
n^a	9	9	9	8	6

^a Defined in text.

Table IV

site	B	C	D	E
A. Equilibrium Constants, $K_{x,y}$, among Aggregates of <i>n</i> -Propyllithium, 253 K, in Cyclopentane				
A	0.36	0.21	0.25	1.07
B		0.58		0.47
C			1.20	0.82
D				0.69
B. Equilibrium Constants, $K_{x,y}$, among Aggregates of <i>n</i> -Propyllithium, 197 K, in Cyclopentane				
A	1.05	0.77	0.60	0.36
B		0.73	0.63	0.34
C			0.86	0.44
D				0.55

Table V. Equilibria among *n*-Propyllithium Aggregates, ΔH and ΔS Values

	$\Delta H_{x,y}$, kcal/mol RLi				
	A	B	C	D	E
A		-1.7	-1.7	-1.3	-0.9
B	-8.2		0.0	0.3	0.8
C	-9.2	-0.9		0.4	0.8
D	-7.4	-0.7	1.8		0.4
E	-6.6	1.6	2.6	0.8	

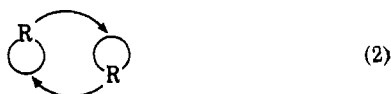
teraggregate exchange processes involving different species take place at different rates.

The multiplicity of the splitting within each resonance and the relative intensities of the peaks within the multiplets are consistent with, *vide supra*, a species undergoing fast intraaggregate carbon–lithium bond exchange. The eventual fading of this fine structure on further cooling implies a slowing down of the internal exchange. However, the expected spectra for slowly rearranging aggregates are not observed, either because the exchange rate is still too fast or the viscosity becomes too large at the lowest temperature to allow observation of fine structure.

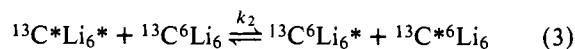
The lithium-6 spectra of the species *n*-propyllithium- ^{1-12}C - ^6Li show effects from lithium exchange among different species. In sum, *n*-propyllithium at equilibrium undergoes two

rapid carbon–lithium bond exchange processes, one between RLi aggregates and a second, much faster process within aggregates. The latter process is still fast, relative to the NMR time scale, by 180 K.

A simplified treatment of the intermolecular exchange can be made by using the ^{13}C NMR line shapes for C_1 of **4** over the temperature range in which hexamer predominates. We consider the overall carbon–lithium bond exchange process to involve the mutual exchange of two propyl groups between two hexamers. As far as the ^{13}C NMR of C_1 of **4** is concerned, process 2 may be modeled as one in which a ^{13}C coupled



equally to six lithium-6 atoms ($I = 1$) exchanges places with another ^{13}C similarly situated in another aggregate, or



Density matrix equations

$$\dot{\tilde{\rho}} = -i[\overline{\mathcal{H}}, \tilde{\rho}] + \tilde{\rho}/T_{\text{OD}} + E\tilde{\rho} \quad (4)$$

for the hypothetical molecule $^{13}\text{C}^6\text{Li}_6$ undergoing exchange process 3 were derived in the product representation using the permutation of indexes (PI) method based on the density matrix theory for NMR line shapes of exchanging systems.¹³ T_{OD} is just the phenomenological line width parameter. The Hamiltonian contains the ^{13}C and ^6Li shifts and ^{13}C – ^6Li coupling constant, under the weak coupling approximation.

To calculate the C_1 absorption, one needs all elements of the density matrix diagonal in $^6\text{Li}_6$ and off-diagonal in ^{13}C :

$$\langle m|\tilde{\rho}|n\rangle = \langle \alpha\phi_i|\tilde{\rho}|\beta\phi_i\rangle \quad (5)$$

where

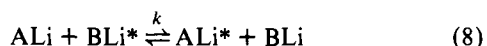
$$\phi_i = \prod_{i=1}^{i=6} \phi_{i_i} \quad (6)$$

ϕ_i is the product function for six lithium-6 atoms, label i . One takes the appropriate $\langle m|\tilde{\rho}|n\rangle$ elements of the density matrix equation. Fortunately, the resulting 728 equations can be simplified by summing all equations for which the ϕ_i 's in (5) have the same $\sum_i m_{z_i} = M$ value and similarly redefining the density matrix elements:

$$\tilde{\rho}_M = \sum \langle \alpha\phi_{i(M)}|\tilde{\rho}|\beta\phi_{i(M)}\rangle \quad (7)$$

The density matrix elements are summed in 13 groups of 1, 6, 21, 50, 90, 126, 140, 126, 90, 50, 21, 6, and 1 each for M values of 6, 5, 4, 3, 2, 1, 0, -1, -2, -3, -4, -5, and -6, respectively. For instance, when $M = 5$, there are six product functions, ϕ_i . The resulting 13 coupled equations are solved in the usual way¹⁴ using computer program SPECTRAL¹⁴ where input is the fluxionally averaged $J(^{13}\text{C}$ – $^6\text{Li})$, $1/T_{\text{OD}}$ (the line width), and the frequency. Comparison of experimental with calculated line widths yields the result that $\Delta H^\ddagger = 4.3$ kcal and $\Delta S^\ddagger = -36$ eu (see Table VI) for the interaggregate exchange process. These parameters are quite similar to values for exchange among diastereomeric aggregates of 2-methylbutyllithium, based on high-field ^1H NMR line shapes.⁶

Line-shape analysis of the ^6Li NMR was accomplished by using a model in which lithium exchanges among magnetically nonequivalent aggregates via bimolecular steps



where A and B represent the entire aggregate save for the last lithium. The mean lifetime of a ^6Li at site N before exchange

to site M is

$$1/\tau_{N \rightarrow M} = k(M) \quad (9)$$

and the exchange contribution to the density matrix equation is

$$E\rho^N = \sum_{\substack{M \\ M \neq N}} k(M)(\rho^M - \rho^N) \quad (10)$$

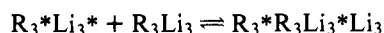
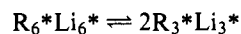
where ^6Li in aggregate N exchanges to four other magnetically nonequivalent sites, M . All these second-order rate constants are taken to be the same and the quantities (M) represent total concentrations of ^6Li in aggregate M . The latter were assigned from the ^{13}C spectra since ^{13}C resonances for different aggregates do not average below 255 K.

Finally, a set of five coupled density matrix equations is compiled for ^6Li in the five kinds of aggregates. This has the appearance of a five-site uncoupled exchanging system. The treatment produces the line shapes shown, together with the experimental ones, in Figure 4. Table VI lists the results of both ^{13}C and ^6Li NMR line-shape analysis.

In the temperature range wherein both ^{13}C and ^6Li line shapes can be used, the rate constants needed to fit the spectra of n -propyllithium are remarkably similar. This implies that the same mechanism is responsible for exchanging alkyl groups and lithiums among aggregates, as might be expected. The results (Figure 5), ΔH^\ddagger and ΔS^\ddagger , are 4.3 kcal and -36 eu from the ^{13}C NMR data and 4.0 kcal and -37 eu from the ^6Li spectra.

At this point it is appropriate to comment on the significance of these NMR line shape fits. Where the ^{13}C line shape is most sensitive to the rate constant, the dominant species is hexamer, so the detected exchange of alkyl groups is between hexamers. The ^{13}C line shape analysis yields the mean residence time of a propyl group in a hexamer. In contrast, the ^6Li line shapes were determined for a sample of propyllithium 96% ^6Li and only natural abundance ^{13}C at C_1 of propyl. There is no contribution from ^{13}C – ^6Li coupling. The ^6Li line shape analysis produces the mean lifetimes of ^6Li atoms between particular exchanges among different aggregates. Clearly, these lifetimes are most likely quite different from one another. By choosing to assume that the lifetimes are given by eq 9, we can reproduce the experimental ^7Li line shapes.

Thus, qualitatively, the line-shape changes observed are the result of the exchange of alkyl groups and lithiums between fluxional aggregates. This has been modeled as taking place in one step via an exchange between aggregates. However, a dissociation–recombination mechanism, first proposed by Brown¹⁵ between hexamer, tetramer, and trimer or between hexamer and trimer (the latter in low concentration) would also move RLi from one aggregate to another and produce the same line-shape changes as the model first described. Thus, line-shape analysis does not distinguish between the two mechanisms. However, the large negative entropy of activation does support the biaggregate exchange step.



Further interpretation of the above results requires some knowledge of the structures of alkyllithium clusters. Since we are dealing with fluxional aggregates, the NMR data do not provide any information on this point. However, the results do provide detailed insight into dynamic processes involving carbon–lithium bond exchange as well as on the association numbers of the aggregates.

Table VI. Summary of Exchange Data for *n*-Propyllithium from ^{13}C and ^6Li NMR

T, K	$k(^{13}\text{C})$	T, K	$k(^6\text{Li})$
205	1.0	180	0.3
226	4.0	196	0.9
235	10.0	214	2.9
252	15.0	230	5.1
298	40.0	244	6.0
		259	9.5

This paper demonstrates the utility of ^6Li and ^{13}C NMR of an enriched alkyl lithium compound. Further applications of this powerful technique are currently under study.

Experimental Section

NMR Equipment. A Bruker WH270 multinuclear NMR spectrometer with Nicolet 1180 computer and disk system was used in the FT mode to obtain ^{13}C and ^6Li spectra with simultaneous proton decoupling, 270 MHz.

^{13}C NMR was accomplished at 67.887 MHz with ~ 200 pulses of 10- μs duration ($<40^\circ$ flip) repeated every 2.719 s. A 16K (16 384 words) transform was carried out over a spectral width of 3000 Hz.

Approximations to generate derivative spectra for resolution enhancement were obtained by offsetting the absorption spectrum in computer memory by several data points and then subtracting from the original spectrum. This procedure has been shown to be related¹⁶ to the technique of multiplying the free-induction decay by a "sine bell" function.¹⁷ As a rule, the spectra were offset by two or three data points before subtraction.

^6Li NMR was carried out at 38.730 223 MHz with ~ 50 pulses of 15–20 μs , repeated every 16.384 s. A 16K transform was used with spectral width of 500 Hz. Both phase-alternating pulse-sequencing (PAPS) and quadrature detection were used to improve the signal/noise ratio.

Relaxation measurements for T_1 were accomplished using the inversion recovery technique, delay- 180° - τ - 90° at 192 K.

Propionic Acid- $1\text{-}^{13}\text{C}$. Ethylmagnesium bromide was prepared from bromoethane (7.3 g, 0.087 mol) and magnesium turnings (1.62 g, 0.067 mol) in 75 mL of diethyl ether. The apparatus consisted of a 500-mL three-neck round-bottom flask equipped with addition funnel (topped by a condenser), overhead Teflon paddle stirrer, and CO_2 inlet. A round-bottom flask with attached addition funnel and side arm bearing stopcock served as CO_2 generator. Carbon dioxide leaving the side arm was dried with a U-tube trap cooled by dry ice/2-propanol and then passed into the inlet neck of the Grignard reaction vessel. Short of the inlet was an attached Hg U-tube manometer.

The apparatus was flamed out under a current of argon and then evacuated to about 250 mmHg pressure. Carbon dioxide (^{13}C) was generated by slow dropwise addition of concentrated sulfuric acid to powdered barium carbonate (^{13}C , 91%, 12 g, 0.060 mol), with stirring. The apparatus was filled with $^{13}\text{CO}_2$ gas to a pressure of ca. 650 mmHg. The Grignard solution was transferred to the dropping funnel and introduced dropwise into the 500-mL three-neck flask at -10°C with stirring. More $^{13}\text{CO}_2$ was generated alternating with the addition of the Grignard solution, keeping the $^{13}\text{CO}_2$ pressure at ca. 650 mmHg. At no time was the internal pressure allowed to exceed 675 mmHg. After the addition of $^{13}\text{CO}_2$ and Grignard was completed, the system was allowed to stir for 15 min. The reaction mixture was hydrolyzed with concentrated aqueous HCl and water. The pH of the water phase was adjusted to 6. This mixture was continuously extracted with diethyl ether for 72 h. Fractional distillation of this extract through a 10 by 1.5 cm column packed with glass helices removed most of the solvent. Pentane was added to the concentrated ether solution, and the mixture was dried over MgSO_4 and fractionally distilled (pentane azeotroped out any remaining water). Final distillation was accomplished through a short-path condenser and product was collected over the range 110–140 $^\circ\text{C}$. A total yield of 3.77 g (84%) of propionic acid was collected, based on barium carbonate. NMR data are listed in Table I.

1-Propanol- $1\text{-}^{13}\text{C}$. A solution of propionic acid- $1\text{-}^{13}\text{C}$ (2.15 g, 0.0286 mol) in 10 mL of freshly dried THF was slowly dropped into an ice-cold slurry of lithium aluminum hydride (1.56 g, 0.0411 mol)

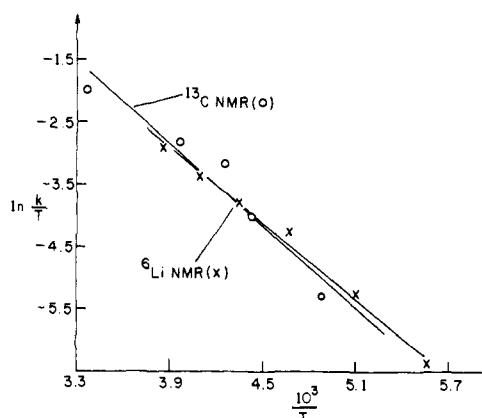


Figure 5. Eyring plots for carbon-lithium bond exchange from ^{13}C and ^6Li NMR.

in 50 mL of dry THF over a period of 30 min. On completion of this addition, the reaction mixture was warmed to room temperature and stirred for 20 h. The excess lithium aluminum hydride was hydrolyzed by slow addition of 10 mL of 20% aqueous potassium tartrate solution. More water and ether were added to this mixture and the system was continuously extracted into ether for 62 h. The extract was dried over MgSO_4 and fractionated through a column, 10 by 1.5 cm, of glass helices. The higher boiling residue was distilled through a short-path system to give 1.43 g of product, bp 95–100 $^\circ\text{C}$ (760 Torr), in 82% yield. NMR data are listed in Table I.

1-Chloropropane- $1\text{-}^{13}\text{C}$. To a solution of hexachloroethane (4.66 g, 0.020 mol) and triphenylphosphine (5.17 g, 0.020 mol) in 25 mL of mesitylene contained in a 100-mL round-bottom flask was added with stirring 1-propanol- $1\text{-}^{13}\text{C}$ (0.93 g, 0.015 mol). Immediately after the addition, a short-path condenser with distillate receiver was attached to the above reaction vessel. Several milliliters of mesitylene were introduced into the pot which was then cooled to 0 $^\circ\text{C}$ with ice water. The reaction mixture was heated to boiling. After 1.5 h, 1-chloropropane had distilled out and mesitylene had begun to distill. Heating was discontinued when the stillhead temperature reacted the boiling point of mesitylene. The 1-chloropropane and mesitylene were then dried and neutralized with solid sodium carbonate and MgSO_4 with swirling until gas evolution ceased. Distillation gave 0.83 g of 1-chloropropane- $1\text{-}^{13}\text{C}$ in 67% yield. NMR data are listed in Table I.

1-Bromopropane- $1\text{-}^{13}\text{C}$. To a round-bottom flask cooled to 0 $^\circ\text{C}$, containing a magnetic stir bar, carbon tetrabromide (11.9 g, 0.036 mol), and triphenylphosphine was added 1-propanol- $1\text{-}^{13}\text{C}$ (1.93 g, 0.0316 mol). A short-path condenser with preweighed receiver was immediately attached to the neck of the flask. The ice bath was removed and the reaction mixture allowed to warm slowly to room temperature. *Note: an exothermic reaction ensued.* The contents of the flask were heated, with vigorous stirring, until liquid refluxed in the neck of the flask. The mixture was allowed to reflux for 1 h. Then the temperature was increased to allow 1-bromopropane to distill over into the collection flask and cooled to 0 $^\circ\text{C}$. Altogether, 3.85 g was collected of material consisting of 1-bromopropane and HBr. This mixture was swirled with several milliliters of saturated aqueous sodium bicarbonate until evolution of CO_2 ceased. The 1-bromopropane was pipetted out of the mixture, dried with P_2O_5 , and distilled, giving 3.3 g of product in 84% yield.

Propyllithium- $1\text{-}^{13}\text{C}$ - $1\text{-}^6\text{Li}$. The apparatus consisted of a two-neck 10-mL pear-shaped flask containing a magnetic stir bar. One neck was fitted with a 2-mm straight-bore stopcock on a side arm protected by a serum cap. The other neck was closed with a glass stopper. This system was flamed out under vacuum and then flushed with dry argon. Cyclopentane (2 mL), freshly distilled from lithium aluminum hydride, was syringed into the flask via the stopcock. A rod of lithium-6 (96%, Oak Ridge National Laboratory) was cleaned with 2-propanol and then cyclopentane. Fresh scrapings of ^6Li (0.08 g, 0.013 mol), obtained under cyclopentane, were rapidly dropped into the flask through the stoppered opening under a current of argon. The mixture in the flask was allowed to stir for several minutes. Then all the cyclopentane was removed by syringe through the stopcock side arm and replaced by dry, oxygen-free cyclopentane. This process was repeated two times. The last 3-mL aliquot of cyclopentane was left in the flask.

Dry, degassed 1-halopropane-*l*-¹³C (0.63 g, 0.0049 mol) was introduced by syringe. The reactant mixture was stirred at room temperature for 14 h, by which time it had turned purple and developed a large amount of finely divided gray solid. The solution was centrifuged and the supernatant liquid transferred by syringe for modified Gilman titration, purification procedures on the vacuum line, and NMR investigation. Modified Gilman titration showed 92% conversion to propyllithium with <2% alkoxide present.

All propyllithium samples were evacuated to a solid on the vacuum line to remove unreacted halide and coupling products. In certain cases propyllithium was distilled across an inverted Y-shaped tube protected at the stem with a straight-bore stopcock. Pure cyclopentane was distilled into the receiver side of the Y and this solution transferred via syringe to the 8-mm NMR tube, protected by a straight-bore stopcock. This assembly was transferred to the vacuum line, and the solution degassed by four freeze-thaw cycles and then sealed off.

Acknowledgment. This research was supported by the National Science Foundation, Grant CHE76-10909A02.

References and Notes

- (1) (a) The Ohio State University. (b) Eastman Kodak.
- (2) Margerison, D.; Newport, J. P. *Trans. Faraday Soc.* **1963**, *59*, 2058-2063.

- (3) Wakefield, B. J. "The Chemistry of Organolithium Compounds"; Pergamon Press: Oxford, 1974.
- (4) Witanowski, M.; Roberts, J. D. *J. Am. Chem. Soc.* **1966**, *88*, 737-741. Fraenkel, G.; Dix, D. T.; Carlson, M. J. *Tetrahedron Lett.* **1968**, 579-582.
- (5) Brown, T. L. *Adv. Organomet. Chem.* **1965**, *3*, 365-395.
- (6) Fraenkel, G.; Beckenbaugh, W. E.; Yang, P. P. *J. Am. Chem. Soc.* **1976**, *98*, 6878-6885.
- (7) McKeever, L. D.; Waack, R.; Doran, M. A.; Baker, E. B. *J. Am. Chem. Soc.* **1968**, *90*, 3244; **1969**, *91*, 1057.
- (8) McKeever, L. D.; Waack, R. *Chem. Commun.* **1969**, 750-751. Bywater, S.; Lachance, P.; Worsfold, D. J. *J. Phys. Chem.* **1975**, *79*, 2148-2153.
- (9) Beckenbaugh, W. E.; Geckle, J. M.; Fraenkel, G. *Chem. Scr.*, in press. Van Dongen, J. C. P., Ph.D. Thesis, University of Utrecht, 1974.
- (10) Fraenkel, G.; Fraenkel, A. M.; Geckle, M. J.; Schloss, F. *J. Am. Chem. Soc.* **1979**, *101*, 4745-4747.
- (11) (a) Pople, J. A.; Schneider, W. G.; Bernstein, H. J. "High Resolution Nuclear Magnetic Resonance"; McGraw-Hill: New York, 1961; p 480. (b) Wehrli, F. *J. Magn. Reson.* **1978**, *30*, 193-209. *Org. Magn. Reson.* **1978**, *11*, 106.
- (12) Zerger, R.; Rhine, W.; Stucky, G. *J. Am. Chem. Soc.* **1974**, *96*, 6048-6055. Schaaf, T. F.; Butler, W.; Gullick, M. D.; Oliver, J. P. *Ibid.* **1974**, *96*, 7593-7594.
- (13) Kaplan, J. I.; Fraenkel, G. *J. Am. Chem. Soc.* **1972**, *94*, 2907-2912.
- (14) Computer program, SPECTRAL ANALYSIS, Instruction and Research Computer Center, The Ohio State University, 1977.
- (15) M. Y. Darensbourg, B. Y. Kimura, G. E. Hartwell, and T. L. Brown, *J. Am. Chem. Soc.* **1970**, *92*, 1236-1242.
- (16) Guéron, M. *J. Magn. Reson.* **1978**, *30*, 515.
- (17) DeMarco, H.; Wüthrich, J. *J. Magn. Reson.* **1976**, *24*, 201.

³¹P Nuclear Magnetic Resonance Studies of Polymer-Anchored Rhodium(I) Complexes

Aart J. Naaktgeboren, Roeland J. M. Nolte, and Wiendelt Drenth*

Contribution from the Department of Organic Chemistry of the University, 3522 AD Utrecht, The Netherlands. Received April 18, 1979

Abstract: Poly(4-diphenylphosphinostyrene) (**1**), poly(4-dicyclohexylphosphinostyrene) (**2**), and poly[1-(4-diphenylphosphinophenyl)ethyliminomethylene] (**3**) were obtained by polymerization of the corresponding monomers. The polymers were treated with (RhClL₂)₂ and with (RhClL'L)₂, where L and L' are ethene and 1,5-cyclooctadiene, respectively. These complexes were added stepwise and during this process the ³¹P NMR spectra were observed. ³¹P chemical shifts and ¹⁰³Rh-³¹P coupling constants were compared with those of monomeric analogues which were treated in the same way.

Recently, considerable interest has been shown in the anchoring of homogeneous catalysts to organic polymers.^{1,2} For instance, polymer-bound rhodium complexes have been synthesized and used as hydrogenation catalysts. Apart from a recent EXAFS study³ concerning the catalytic site of the polymer-bound Wilkinson catalyst, there has been hardly any other study relating to characterization of anchored catalysts.

It has been shown that ³¹P NMR can help to elucidate the structures of metal-phosphine complexes.⁴ Both the ³¹P chemical shift and the metal-phosphorus coupling constant can provide information concerning the stereochemistry of these complexes and their coordination number.

Grubbs et al.⁵ have tried to use ³¹P NMR as a tool for studying polymer-supported rhodium complexes, but failed to observe any signals of coordinated phosphines. They attributed this failure to increased relaxation times due to complexation of the phosphine to the metal center. We consider this explanation to be less likely, because without rhodium the phosphine in polystyrenes gives a clear ³¹P NMR signal⁵⁻⁷ and therefore will have normal relaxation time, while coupling to rhodium is expected to decrease rather than increase the relaxation time.⁸

So far,² nearly all supports used to anchor homogeneous catalysts have a low phosphorus content and phosphine is un-

evenly distributed over the polymer chain. This is very unfavorable for a ³¹P NMR study because the signal strength is low and appreciable variations occur in the environment of the phosphorus in the polymer. Therefore, we prepared three polymers which have a phosphine function in each repeating unit: poly(4-diphenylphosphinostyrene) (**1**), poly(4-dicyclohexylphosphinostyrene) (**2**), and poly[1-(4-diphenylphosphinophenyl)ethyliminomethylene] (**3**). These polymers were obtained by polymerization of their phosphine-containing monomers. Polymers **1** and **2** will have a more or less random

